Article citation info:
Bozali B. 2026. Investigation of Frequency Dependent Electrical and Dielectric Properties of Maple Wood (*Acer Trautvetteri* Medw.) with Different Surface Treatments. *Drewno. Prace naukowe. Doniesienia. Komunikaty* 69 (217): 00072. https://doi.org/10.53502/wood-211284

Łukasiewicz Poznań Institute of Technology

Drewno. Prace naukowe. Doniesienia. Komunikaty
Wood. Research papers. Reports. Announcements

Journal website: https://drewno-wood.pl

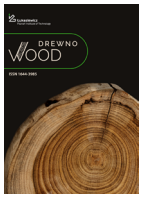

Investigation of Frequency Dependent Electrical and Dielectric Properties of Maple Wood (*Acer Trautvetteri* Medw.) with Different Surface Treatments

Beytullah Bozali *

Department of Electricity and Energy, Düzce University, Düzce, Turkey

Article info
Received: 28 August 2025
Accepted: 25 September 2025
Published: 15 December 2025

Keywords
maple wood
dielectric properties
frequency-dependent behavior
complex impedance
electric modulus

In this study, the electrical and dielectric properties of maple wood (Acer trautvetteri Medw.) were comprehensively investigated under three different surface conditions: untreated control (CW), two-week water immersion (SW), and double varnish (VW), as well as a function of frequency. For the accuracy of electrical analysis, all test samples were evaluated in a dry state and comparative analysis was performed between surface treatment groups. In the experimental analyses in the frequency range from 100 Hz to 1 MHz, reel/imaginary part of dielectric permittivity (ε′ and ε″), dielectric loss factor (tanδ), alternating current electrical conductivity (σac), specific heat capacity (C), conductivity-dependent free energy component (G/ω), and real (Z′) and imaginary (Z″) impedance components were comprehensively evaluated. According to the test results, the SW test samples, with their high (ε′) and (ε″) values, were found to provide significant ionic and dipolar contributions. However, due to their high (tanδ) and (σac) values, their energy storage capacity is limited, and their conductivity potential is high. The VW test samples, with their low (ε″) and (tanδ) values, exhibit strong insulating properties, making them suitable for high-frequency capacitive applications. The CW test samples, in contrast, exhibit a balanced conductivity-insulation profile with moderate dielectric response. Impedance analyses (Z′, Z″) revealed that the low-resistance ion transport mechanism dominates in the SW test samples, while the surface coating creates a high-resistance barrier, thus limiting charge transport in the VW test samples. The (G/ω) results indicate high energy dissipation in the SW test samples over a wide frequency range, while the VW test samples exhibit stable storage behavior with low energy loss. According to the test results, maple wood, depending on the surface treatment, has potential for use in sensor technologies (SW), radiofrequency isolating components (VW), and general structural dielectric applications (CW), and allows for targeted performance engineering through material modification.

DOI: 10.53502/wood-211284
This is an open access article under the CC BY 4.0 license:
https://creativecommons.org/licenses/by/4.0/deed.en.

Introduction

The dielectric characteristics of non-conductive materials are associated with their polarization behavior under an external electric field. Properties determine the electrical energy storage capacity of a material and the mechanisms of energy loss. Electrical conductivity and dielectric properties are directly related to the physical structure and moisture content of wood. Properties serve different functions in fresh and dry wood. Electrical properties, which are affected by the moisture content, ionic conductivity, and structural anisotropy of wood, play an important role in understanding wood physiology and developing non-destructive testing

* Corresponding author: beytullahbozali@duzce.edu.tr

techniques in wood processing [Ghildiyal et al. 2025]. The literature reports on a significant relationship between dielectric constant and thermal conductivity. In this context, energy efficiency refers to wood's ability to resist heat transfer, i.e., reducing heat loss. This relationship could contribute to the development of new and rapid methods for assessing wood's in-situ thermal performance [Saeed, 2022].

The physical structure and moisture content of wood have been shown to be directly related to its electrical conductivity and dielectric properties. The differential effects of properties on fresh and dry wood are important parameters for understanding the electrical behavior of the material [Zhang and Zhou, 2023]. Electrical properties, defined by moisture content, ionic conductivity, and structural anisotropy, provide a solid basis for the development of non-destructive testing methods for understanding wood physiology and evaluating wood processing [Varada Rajul and Mohanty, 2016].

Heat treatment with oil, an environmentally friendly modification method, is proving to be an effective approach for improving the physical, chemical, and mechanical properties of wood. Studies in the literature indicate that treatment with heated vegetable oils offers superior properties compared to traditional methods and offers significant sustainability potential [Mandraveli et al. 2024].

Monitoring the moisture content of porous, hygroscopic building materials using electrical methods contributes significantly to the evaluation of their thermal and electrical properties [Otten et al. 2017]. The influence of frequency on dielectric properties can significantly affect the electromagnetic response of wood, especially during changes in moisture content. In this study, maple was chosen as a suitable analytical material due to its unique physical structure, wide industrial application range, and dielectric strength. The literature shows that maple is sensitive to structural and compositional changes after thermal and chemical treatment. This provides an excellent example for understanding the frequency-dependent dielectric properties of lignocellulosic structures [Dzurenda et al. 2020; Výbohová et al. 2018].

Maple (*Acer troutveteri* medw) wood has anisotropy enhancement of 1.79, density of 591.76 kg/m^3, volume expansion of 10.99%, radial expansion of 3.38%, and elongation of state. 89.24% after two weeks, fiber content of 18.56% and electrical thermal conductivity 0.151 W/mK [Ayata et al. 2019], 25% lignin, 38% cellulose, 20% pentosan [Bozkurt and Erdin, 2013], with a screw bond strength of 39.91 N/mm^2 in the transverse direction, 36.63 N/mm^2 in the transverse 5.9 N/mm^2 direction, the maximum load obtained was 33.45 N/mm^2 [Çavuş and Ayata, 2018]. A high tanδ value indicates large energy losses during the dipole orientation process, while a low tanδ value indicates high dielectric stability and insulating properties of the material [Kao, 2004; Barsoukov and McDonald, 2005].

The main objective of this study was to systematically investigate the electrical and dielectric response of maple wood under three different surface conditions, namely untreated control (CW), two-week water immersion (SW), and double varnish (VW), and in the frequency range from 100 Hz to 1 MHz. The real dielectric permittivity (ε′) represents the electrical energy storage capacity of the material, while the virtual permittivity (ε″) represents energy losses. The dielectric loss factor (tanδ) characterizes the efficiency of the material to store electrical energy with minimum loss. The alternating current conductivity (σac) reflects the mobility of electric charges. The specific heat capacity (C) defines the heat storage capacity of the material. The free energy component (G/ω) represents the energy conversion resulting from conductivity. The real (Z′) and imaginary (Z″) components of the impedance represent the resistance and energy storage responses, respectively. The aim is to determine the effects of surface modifications on material performance based on these parameters. The novelty of this study is to present a comprehensive frequency-based behavior map for maple wood in terms of conductivity and energy storage mechanisms, jointly evaluating specific heat capacity, complex impedance components, dielectric constants, and energy loss parameters. The goal is to help determine the most suitable configuration for sensor, insulator, or energy storage applications, depending on the type of surface treatment.

Materials and methods

Maple (*Acer trautvetteri* Medw.) wood was used as the test sample in this study. Sapwood sections were used, a total of 10 samples for each group. Samples were taken at a diameter of 1.5 meters above ground. Samples were prepared parallel to the fiber direction. The test samples were selected from among visually flawless materials (free of cracks, knots, etc.) before being subjected to the specified surface treatments. Conditioning processes were performed on the test samples [ISO, 1976]. Test measurements of maple wood samples are given in Table 1.

Experimental design: untreated control (CW) test samples were taken from untreated test samples. Two-week water immersion (SW) test samples were stored in distilled water for 2 weeks. Solvent-based, transparent, and glossy wood varnish was used for double varnish (VW) test samples. The varnish has the properties of (colorless; viscosity: 13,000–17,000 sec, 20°C, DIN CUP 4; relative density: 0.83–0.87 g/cm^3; dry to touch: 1–3 h; waiting time between coats: 12 h;

Table 1. Test measurements of wood samples

Wood type	Control Wood (CW) (mm x mm x mm)	Soaked Wood (SW) (mm x mm x mm)	Varnished Wood (VW) (mm x mm x mm)
Maple	250 x 40 x 15	250 x 40 x 15	250 x 40 x 15

full drying time: 12 h). The varnish was applied to the surfaces in two coats, with 12h between coats. Varnishing operations were carried out in accordance with ASTM D3023-98 [2017] standard.

The electric field is defined as the force acting on a unit positive charge and is expressed as a vector quantity. The mathematical expression for the electric field is given in Equation (1).

$$\vec{E} = \frac{\vec{F}}{q} \tag{1}$$

In Equation (1), $\vec{E}$ represents the electric field vector (N/C or V/m) and $\vec{F}$ is the electric force acting on the load, q is defined as the test load.

The rearrangement of charges within the material results in polarization (P) and a decrease in the net electric field. The polarization equation is given in Equation (2).

$$P = \varepsilon_0 X_e E \tag{2}$$

In Equation (2), ε_0 is the gap permittivity, P is the polarization, X_e is the electrical susceptibility, and E is the applied electric field [Bozkurt, 1982].

To perform dielectric spectroscopy (DS) measurements, two opposing surfaces of each test sample were covered with approximately 20 mm wide self-adhesive copper conductive tape. The experimental setup used to perform dielectric measurements on the test samples is shown in Figure 1. In Figure 1, the copper conductive tape was removed 10 mm or more from two opposing surfaces of each test sample to allow for the connection of LCR measurement probes. The copper conductive tapes bonded to both surfaces of the test sample formed a capacitor-like shape, making it susceptible to exposure to an alternating electric field.

Measurements were made at frequencies ranging from 100 Hz to 1 MHz. All dielectric parameters are calculated using the formulas below. Capacitance (C) represents the specific heat capacity of the system, which is directly related to the complex dielectric constant.

$$C = C_0 \varepsilon' \tag{3}$$

$$\frac{G}{w} = C_0 \varepsilon'' \tag{4}$$

In Equation (3), C_0 represents the frequency-dependent capacitance of the composite medium, while the conductivity (G/w) values are represented by Equation (4). In Equation (4), $\omega=2\pi f$ is the angular frequency, (ε') is the real permittivity, (ε'') is the imaginary permittivity, and $C=\varepsilon_0\varepsilon_r A/d$ is the geometric capacitance. Dielectric constants ε_0 and ε_r represent the measured contact area of the composite medium A, and d represents the thickness of the composite medium [Wei et al. 2016; Demir, 2025]. In Equations (3) and (4), the frequency-dependent behavior of the

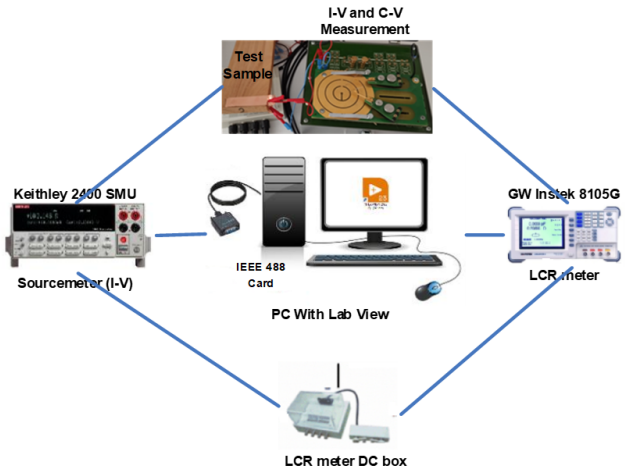

Fig. 1. DS measurement system used in the study [İbrahimoğlu et al. 2024; Demir et al. 2024; Ramazanoğlu et al. 2025b]

specific heat capacity (*C*) is indirectly related to the change of (ε′ and ε″) [Kao, 2004].

The complex impedance approach is widely used in dielectric analysis to evaluate the electrical response of a material with both resistive and reactive components. The complex impedance Z^* is defined as the sum of the real Z′ and imaginary Z′ components. The real (ε′) and imaginary (ε″) components of the dielectric constant are generated using Equations (6)–(9), considering the expression for the complex impedance Z* defined in Equation (5) [Gencel et al. 2024; İbrahimoğlu et al. 2024; Kïp et al. 2024; Demir, 2025].

$$Z^* = Z' + jZ'' \tag{5}$$

The complex dielectric constant ε* is expressed as in Equation (6) using the impedance spectrum.

$$\varepsilon^* = \frac{1}{jwZ^*} = \varepsilon' + j\varepsilon'' \tag{6}$$

In Equation (6), the complex permittivity is expressed with ε* and the angular frequency ω=2πf. Using Equation (6), the real (ε′) and imaginary (ε″) complex dielectric constant components are calculated in Equations (7) and (8) [Türk et al. 2020; Kocakülah and Köysal, 2023b]

$$\varepsilon' = \frac{1}{wC_0} \cdot \frac{Z''}{(Z')^2 + (Z'')^2} \tag{7}$$

$$\varepsilon'' = \frac{1}{wC_0} \cdot \frac{Z'}{(Z')^2 + (Z'')^2} \tag{8}$$

$$C_0 = \varepsilon_0 \frac{A}{d} \tag{9}$$

In Equations (7)-(9), C_0 represents the free-space capacitance. In Equation (9), ε_0 (=8.854 × 10^{-12} F/m) represents the dielectric permittivity [Kocakülah and Köysal, 2023a]. Dielectric properties play an important role in material behavior.

Capacitance (*C*) and conductivity (G/ω) measurements obtained depending on frequency change are important in calculating parameters [Kïp et al. 2024; Kırkbınar et al. 2024]. The free energy behavior of materials under alternating current (AC) includes many physical processes such as conductive losses, polarization relaxation, and segmental mobility. Processes are generally associated with (ε″) and expressed by Equation (10).

$$\frac{G}{w} = C_0 \varepsilon'' \tag{10}$$

In Equation (10), *G* is the conductance (S), ω=2πf is the angular frequency (rad/s), $C_0=\varepsilon_0 \cdot A/d$, geometric capacitance, (ε″) is the dielectric loss component [Macdonald, 1992; Barsoukov and Macdonald, 2005; Demir, 2025]. Alternating current (AC) electrical conductivity (σ_{ac}) can be calculated based on the dielectric loss with Equation (11).

$$\sigma_{ac}(w) = \varepsilon_0 w \varepsilon'' \tag{11}$$

Equation (11) represents the angular frequency (rad/s) $\omega=2\pi f$. It can be stated that the free energy distribution is directly related to conductivity and lossy energy mechanisms. In Equation (11), ε_0 represents the dielectric constant of the cavity (8.854×10^{-12} F/m), ω represents the angular frequency, and ε″ represents the loss constant of the dielectric constant. To obtain accurate information about the electrical conductivity of the resulting wood material medium, the equation defining the relationship between (σ_{ac}) and the logarithmic value of the frequency is given in Equation (12).

$$\sigma_{ac} = A.w^s \tag{12}$$

In Equation (12), *A* represents a constant leading factor, and s represents the exponential parameter that determines the frequency-dependent conductivity behavior. The system's conductivity (ε″) varies with frequency. High conductivity indicates a system's tendency to lose energy, while low conductivity indicates its insulating and energy storage capacity [Macdonald, 1992; Barsoukov and Macdonald, 2005; Demir, 2025].

tanδ is an important parameter that indicates the extent to which a system conducts electrical energy with loss. The variation of this energy with frequency can be explained by the dielectric loss factor tanδ. It is an important parameter for determining performance in high-frequency applications and energy conversion systems. The loss factor tanδ is calculated from the real (ε′) and imaginary (ε″) components of the complex dielectric constant (ε* = ε′ – jε″) and is expressed by Equation (13) [Demir, 2025; Ramazanoğlu et al., 2025].

$$\tan\delta = \frac{\varepsilon''}{\varepsilon'} \tag{13}$$

Equation (13) represents the loss component of the system relative to its energy storage capacity and forms the basis for interpreting the electrical stability and resonant behavior of the material. The frequency-dependent tanδ profile is an important parameter for evaluating the effects of parameters such as moisture content, surface coating, and fiber orientation on the material performance, especially for wood samples.

The phase angle dependence of the complex impedance (Z*) in Equation 14, the real and imaginary impedances (Z′ and Z″) in Equations 15 and 16, and Z* (tanθ) in Equation (17) are determined using the following formulas.

$$Z^* = \frac{1}{i\omega C_0 \varepsilon^*} = Z' + jZ'' \tag{14}$$

$$Z' = \frac{\varepsilon''}{\omega C_0 \left[\varepsilon'^2 + \varepsilon''^2\right]} \tag{15}$$

$$Z'' = \frac{\varepsilon'}{\omega C_0 \left[\varepsilon'^2 + \varepsilon''^2\right]} \tag{16}$$

$$\tan\theta = \frac{Z''}{Z'} \tag{17}$$

The equations in Equation (14)-(17) allow us to calculate the impedance components from the dielectric constant measurements and provide additional information about the electrical properties of the maple test samples [Demir et al. 2024; Ramazanoğlu et al. 2025a; 2025b].

Results and discussion

The C-F diagram in Figure 2 shows the variation of the specific heat capacity (*C*) of the edge samples under three different surface conditions (untreated control (CW), two-week water immersion (SW), and double varnish (VW)) with frequency. The specific capacitance (*C*) is directly related to the dielectric constants (ε′, ε″), geometric parameters, and conductivity of the system, as can be seen in Equations (3) and (4). In their study, Ondo-Ndong and colleagues found that the observed decrease in capacitance in the materials is inversely proportional to the increase in conductivity values [Ondo-Ndong et al. 2018].

The CW test sample begins in a low frequency range, at approximately 10^{-9} F, and the capacitance value decreases rapidly to 10^{-11} F with increasing frequency. This finding indicates that the high storage capacity resulting from focused interfacial polarization at the electrode and the accumulation of charge carriers at low frequencies decreases with increasing frequency due to the restriction of dipole mobility and the suppression of polarization mechanisms.

In the SW test sample, the capacitance values exhibit pronounced (resonance-like) peaks in the mid-frequency range up to 10^{-10} F. Similarly, in another study, it was stated that capacity values increased with increasing lignocellulosic material content and there were significant changes in storage properties with frequency [Markiewicz and Paukszta, 2009]. This finding suggests that the high ionic conductivity resulting from the aqueous impregnation of the test sample and the strong contribution of free charge carriers, especially at frequencies around 10 kHz, are due to the orientational polarization of ions and water molecules, which increases the capacitance in this frequency range. However, this contribution decreases with increasing frequency, and the capacitance decreases. The VW test sample showed a low and nearly constant capacitance profile (≈10^{-11} F) across the entire frequency range. The lacquer coating on the test sample inhibits both surface conductivity and moisture transport, thus limiting dipolar and ionic motion. Interfacial polarization was also found to be suppressed, and capacitance values remained low.

When investigating the electrical and dielectric mechanisms, the high capacitance values of the CW test sample indicated dominant interfacial polarization at low frequencies; the peak observed in the SW test

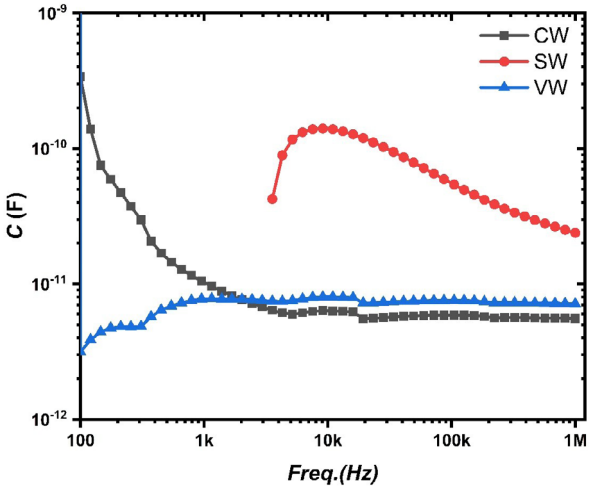

Fig. 2. Capacitance-frequency variation for maple

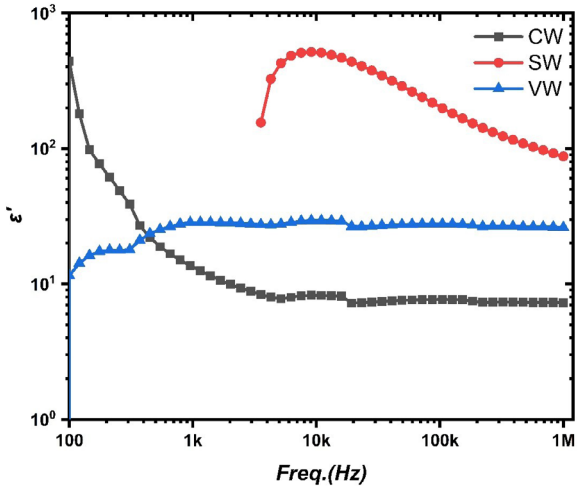

Fig. 3. Frequency-dependent behavior of the real dielectric permittivity for maple

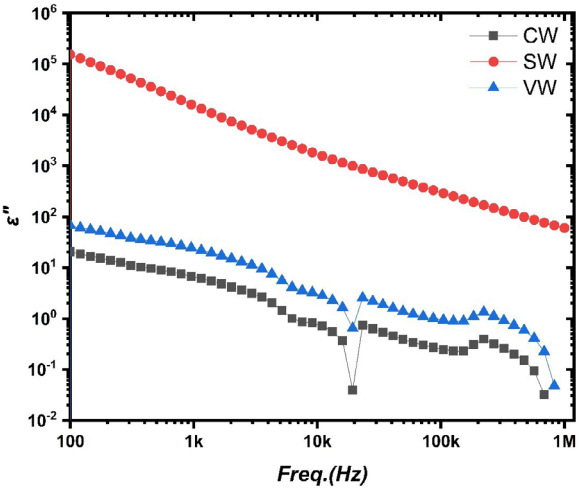

Fig. 4. Frequency-dependent behavior of the imaginary permittivity for maple

sample indicated ionic polarization and the relaxation effect of water molecules; and the low and constant capacitance profile of the VW test sample indicated suppressed polarization mechanisms due to effective surface insulation. Results demonstrate that surface modifications in maple wood allow strong control over dielectric storage behavior and that the SW state offers potential for energy storage applications, as it significantly enhances capacity through ionic doping. Figure 3 presents a detailed analysis of the ε′–f diagram of the samples, the dielectric constant, and the real permittivity (ε′) behavior under three different surface conditions (CW, SW, and VW) and frequencies between 100 Hz and 1 MHz.

The CW test sample has a high ε′ value of approximately 3×10^2 in the low frequency range. However, this value decreases rapidly with increasing frequency, falling below 10.

In the SW test sample, the (ε′) values reach a clear maximum of approximately 3×10^2 in the mid-frequency range, making them significantly higher than those in the CW and VW test samples. Results are attributed to the high ionic conductivity and high orientational dipole density of the water-impregnated structure, which is particularly pronounced at frequencies around 10 kHz. The relaxation effect of ions and water molecules increases the value of (ε′) in this expression. At higher frequencies, the efficiency gradually decreases due to the frequency-limiting polarization process. In contrast, the VW test sample is low and stable (≈20) at all frequencies. The ε' value increases with increasing fiber breakage and the polar property is especially effective at medium frequencies [Markiewicz and Paukszta, 2009]. The addition of water and CNTs to polymer composite systems significantly increases the ε' values [Wang et al. 2022]. The coating layer effectively limits interfacial and dipolar polarization, preventing water loss and surface conductivity. This also significantly reduces the capacity of energy storage under electrical outlets.

Considering the electrical and dielectric properties, the high angle value (ε′) of the CW sample indicates

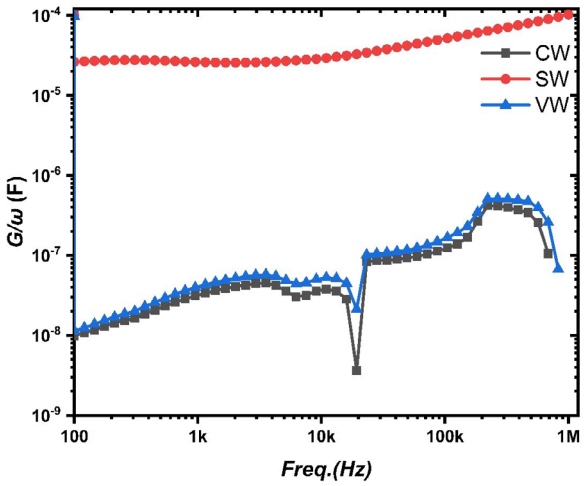

Fig. 5. Frequency-dependent conductance (G/ω) plot for maple

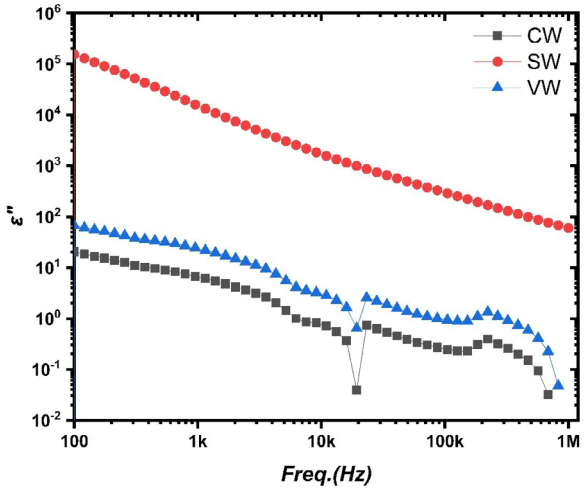

Fig. 6. Frequency-dependent dielectric loss factor (tanδ) behavior for maple

the low-frequency interfacial polarization. The large deviation in the SW-scale model reflects the interaction effect of ionic and dipolar combinations. The compact and stable nature of the VW experimental model demonstrates the suppressive effect of the insulator on the polarization mechanism. Results indicate that the modification of the sample surface can control the energy storage capacity under electric fields, and in particular, the SW-treated test sample can be a high-strength dielectric due to its high efficiency (ε′).

The ε″-f diagrams of the samples shown in Figure 4 investigate the frequency-dependent dielectric loss behavior under three different surface conditions (CW, SW, and VW).

The CW test sample in Figure 4 exhibited a moderate loss profile with (ε″) values starting at approximately 10^1 at low frequencies. With increasing frequency, this value gradually decreases to below 1 Hz. Results indicate that ionic conduction and interfacial polarization dominate at low frequencies, while at high frequencies, the energy loss decreases due to the restricted dipole orientation.

The SW test sample exhibited the highest (ε″) values across the entire frequency range compared to other surface conditions. The values, which start at 10^5 at low frequencies, decrease continuously with increasing frequency and remain above 10^2 even at high frequencies. In another study, it is stated that ε″ values especially peak around 1 kHz, and ion transport in the polymer matrix is effective [Wang et al., 2022]. The high loss is due to the intense ionic contribution in the water-impregnated structure, the high conductivity, and the increased charge carrier mobility. The extremely high (ε″) values, especially in the low-frequency range, indicate that the charges in the electric field cannot change direction quickly, and energy dissipation is increased due to the field effect. The VW test sample exhibits higher (ε″) values at low frequencies than the CW test sample, but significantly lower (ε″) values than the SW test sample. Values, which are around 10^2 at low frequencies, indicate a gradual decrease with increasing frequency. The lacquer layer reduces dielectric losses by limiting surface moisture and ion mobility. Because

the surface is not completely covered, it exhibits slightly higher losses than the CW test sample.

Evaluating the electrical and dielectric mechanisms, the high (ε″) values of the SW test sample indicate its suitability for high-loss power distribution and electromagnetic damping applications. The CW test sample, with its low loss profile, offers advantages in areas requiring insulation properties, while the VW test sample exhibits an intermediate level of performance, providing both limited losses and surface protection.

The G/ω–F diagram shown in Figure 5 examines in detail how the frequency-dependent free energy component (G/ω) changes the energy storage and dissipation capacities of the maple samples under three different surface conditions (CW, SW, and VW).

A gradual increase was observed in the CW and VW test samples, starting at 10^{-8} F in the low frequency range and continuing through the mid-frequency range. This increase indicates that the limited mobility of charge carriers and the polarization effect at low frequencies increase with increasing frequency due to the contribution of interfacial polarization and dipolar relaxation processes.

The VW test sample showed slightly higher G/ω values at all lengths than the CW test sample. This indicates that the film coating contributes to surface charge absorption and energy storage. Both simulations showed significant peak shapes in the high frequency range (≈10^5–10^6 Hz), indicating that the acoustic effects and field–voltage interactions reach their maximum.

On the other hand, the experimental SW gauge showed consistent values over the entire temperature range between 10^{-5} F and 10^{-4} F; rates are several times higher than other ground-based methods. Results indicate that ionization and the saturated water vapor enhancement led to energy storage. In addition, SW is associated with high G/ω values at high energies and the ability to adapt to rapid changes in highly mobile ions.

In addition to the electrical and decoupling properties, the SW model proves to be suitable for high-energy storage and electrostatic energy sequestration due to its high free energy component.

The CW and VW test samples, with their lower G/ω values, demonstrate potential for low-energy-loss insulating systems. VW offers a slight performance improvement compared to CW, leading to improvements in both surface protection and storage capacity.

The tanδ-F plot in Figure 6 details the variation in dielectric loss factor with frequency for the test samples under three different surface conditions (CW, SW, and VW). The loss factor tanδ is an important parameter that indicates how much energy a dielectric material loses relative to its energy storage capacity.

The SW test sample exhibits very high losses at low frequencies, with tanδ >10. However, the CW and VW samples show tanδ <0.1, reflecting the insulating properties of these materials. Similar to literature reports, there is a significant increase in tanδ values in natural fiber reinforced composites exposed to water [Shabnam, 2011]. Hussein and Abdullah noted that tanδ is high in cellulose composites at low frequencies [Hussein and Abdullah, 2017]. This finding indicates that the water-saturated structure exhibits high ionic conductivity and strong dipolar relaxation mechanisms. High losses indicate that a significant portion of the energy stored in the material under the electric field is converted to heat and conduction losses.

The CW and VW test samples exhibit similar tanδ profiles at low frequencies, with the VW test sample exhibiting higher losses in the early frequency ranges compared to the CW sample. This difference is due to the charge-trapping regions created by the surface resistance layer and the effects of interfacial polarization. The tanδ values of both samples decrease significantly toward the mid-frequency range, which is due to dipolar relaxation processes that give way to faster, but lower-amplitude, polarization mechanisms at high frequencies. In the high-frequency range (>10^5 Hz), the SW sample exhibited the highest loss, while the CW and VW samples exhibited constant and low tan δ values in the range of 0.01 to 0.1. Results demonstrate that the CW and VW surface conditions exhibit insulation properties with low energy loss at high frequencies. The VW exhibits similar or lower losses than the CW in this range, suggesting that a paint coating could contribute to improving energy efficiency in high-frequency applications.

In terms of electrical and dielectric mechanisms, the SW sample, with its high loss factor, offers potential for use in highly sensitive dielectric sensing applications, while the CW samples, and especially the VW, due to their low losses, are better suited for high-frequency capacitive energy storage and applications with insulating materials.

The (σ_{ac}–F) plot in Figure 7 examines in detail the frequency-dependent behavior of the alternating current electrical conductivity (σ_{ac}) of edge samples under three different surface conditions (CW, SW, and VW). The equations for alternating current electrical conductivity (σ_{ac}) are given in Equations (11) and (12). (σ_{ac}) refers to the ability of a material to conduct free energy losses under an electric field by current. In dielectric systems, (σ_{ac}) reflects the resistive energy component of the system and indicates the extent to which free energy is conserved or lost. A high conductivity (σ_{ac}) indicates the system's tendency to lose energy, while a low conductivity indicates its insulating and energy storage capacity [Macdonald, 1992; Barsoukov and Macdonald, 2005; Demir, 2025].

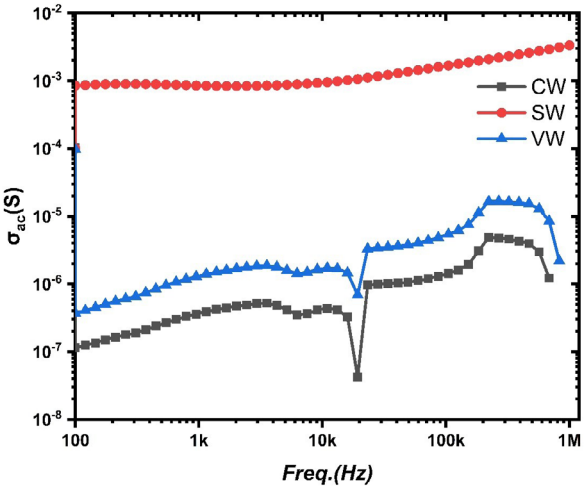

Fig. 7. Frequency-dependent variation of AC electrical conductivity for maple

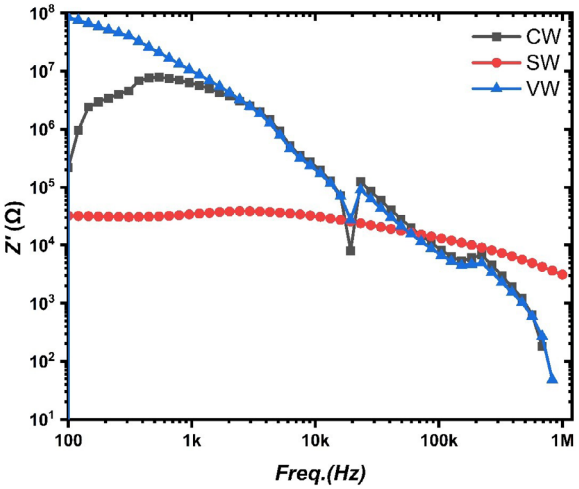

Fig. 8. The real impedance (Z′) for maple

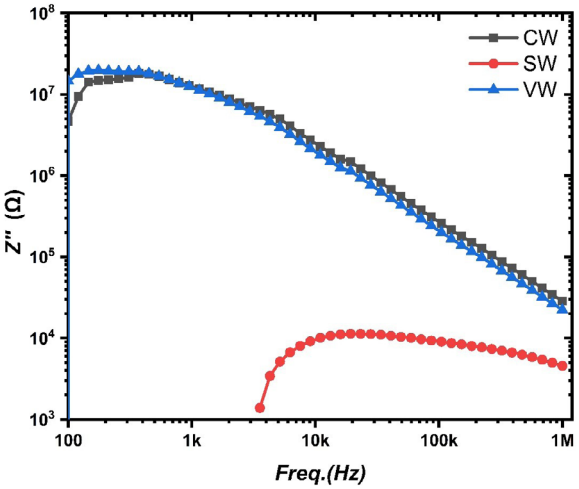

Fig. 9. The imaginary part of impedance (Z″) for maple

In the frequency range (100–1000 Hz), the SW test sample showed constant conductivity at ~10^{-3} S, thus reaching its highest conductivity values. This finding is due to the high density of mobile ions in the water-saturated sample, making ionic conduction the dominant mechanism. This stable and high conductivity of SW indicates that the material converts a large portion of its free energy into

electrical conduction, resulting in low energy storage capacity.

The CW and VW test samples showed lower conductivity values at lower frequencies. The CW test sample showed conductivity values at ~10^{-7} S, while the VW test sample showed higher conductivity values (~10^{-6} S) due to the surface coating. Previous studies have indicated that the lignocellulosic structure exhibits an increase in σac with both water content and frequency [Markiewicz and Paukszta, 2009]. In addition, it has been stated that σac increases with ionic doping in fullerene-doped films [Hussain et al. 2022]. The lacquer layer partially supports ion mobility at low frequencies by increasing surface polarization and has been shown to be generally insulating. A gradual increase in conductivity values was observed for the CW and VW test samples across the entire frequency range (1 kHz to 100 kHz). This increase is due to the increase in AC conductivity due to dipolar relaxation and surface polarization in dielectric systems. The SW test sample, on the other hand, maintained a high and constant level of conductivity in this range and showed a weak frequency dependence.

In the frequency range (>100 kHz), both the CW and VW test samples showed a significant increase in conductivity. The VW test sample showed higher conductivity than the CW test sample due to the surface coating. This finding is because the resistive layer facilitates the transient movement of charge carriers at high frequencies, which improves the conduction mechanism. The SW test sample, on the other hand, exceeded 10^{-3} S value and exhibited strong conductivity even at high frequencies. When evaluating the electrical and dielectric mechanisms, the SW test sample proved suitable for moisture sensing or conductive fill applications due to its high AC conductivity, while the CW and, especially, VW test samples were more suitable for high-frequency insulation and capacitive energy storage applications due to their low conductivity.

The Z′ data for the maple wood species shown in Figure 8 were examined in detail at various frequencies under three different surface conditions (CW, SW, and VW). In the frequency range (100–1 kHz), the VW test sample exhibits the highest Z′ value at ~10^8 Ω, thus demonstrating a strong insulating character. This finding is because the lacquer coating on the surface significantly restricts the movement of ions and dipoles and prevents the transfer of charge carriers under electric fields.

On the other hand, the CW test sample exhibits a lower, but still high, impedance in this range of ~10^7 Ω. Being saturated with water, the SW sample exhibited the lowest impedance values of 10^4 Ω, indicating dominant ionic conductivity. In their study on glass structures, Teja and colleagues stated that Z' values decreased significantly because of conductive additives [Teja et al. 2012]. While the VW and CW models show a significant decrease in Z values over the frequency range (1–100 kHz), the SW model shows a relatively stable, low-impedance profile. This indicates that the decrease in Z′ values in CW and VW samples is due to dipole relaxation and charge distribution at the interface, which led to a decrease in resistance.

A decrease in Z′ values was observed in all samples over the entire frequency range (>100 kHz). Furthermore, it was observed that the VW model maintained corrosion properties during this period and showed higher impedance values compared to the CW model. However, the SW model shows low impedance due to high permeability and a slight decrease in ions with increasing frequency. To distinguish between electrical and dielectric devices, the VW model, with its high impedance, is suitable for electrical insulation, while the SW model, with its low impedance and high conductivity, is suitable for humidity sensing or measurement. However, the CW model provides a balance between two properties and can be used in systems that require moderate insulation and have limited conductivity.

The Z″–F diagram of the sample in Figure 9 summarizes the variation of impedance (Z″) with frequency for three different surface conditions (CW, SW, and VW).

In the high frequency range (100-1 kHz), CW and VW signals showed high Z″ values up to 10^7, indicating good energy conservation and efficiency. In their study, Saini and Arora found that the decrease in Z″ values in the high frequency range was due to the users' inability to fully adapt to the electric field [Saini and Arora, 2012]. Large effects are because charged carriers (ions or dipoles) move with the electric field, creating large changes in the electric field, especially at high frequencies. The VW sample exhibits slightly higher values than the CW sample due to the surface coating, suggesting that surface insulation increases the lifetime of the energy storage device.

The SW test sample, on the other hand, has low Z″ values of only ~10^4–10^4 Ω in the low frequency range. This finding suggests that the water-saturated structure enhances the ionic conduction mechanism, resulting in the rapid conversion of stored energy into conduction and a reduction in phase lag. In the frequency range (1k-100 kHz), the CW and VW test samples show a similar trend, with a gradual decrease in Z″ values. This decrease can be explained by the fact that charge carriers cannot fully keep up with field changes as the frequency increases, resulting in a partial loss of stored energy. However, the SW test sample shows a slight peak in this frequency range, indicating that the ions undergo maximum energy deceleration at a certain relaxation frequency.

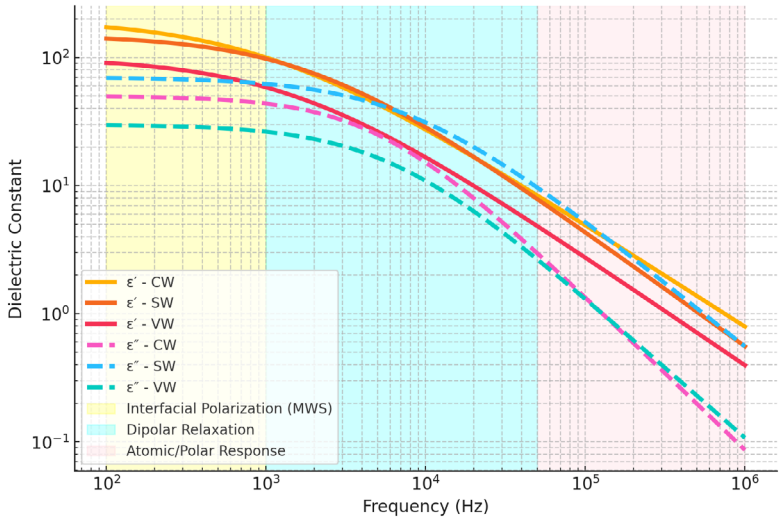

Fig. 10. ε′–ε″ graph for maple wood

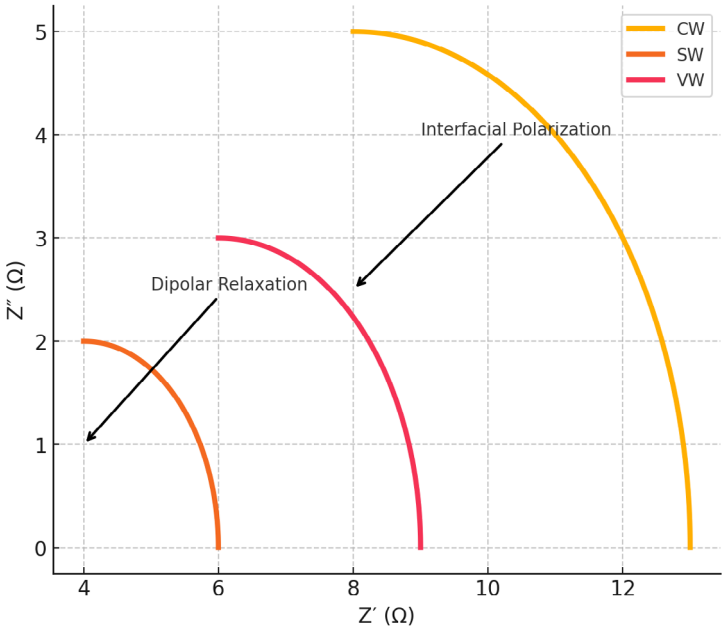

Fig. 11. Nyquist (Z′–Z″) spectrum graph for maple wood

In the frequency range (>100kHz), the Z″ values of all test samples decrease significantly, and the storage capacity decreases, leading to the dominant conduction mechanism. Even at frequencies, the VW test sample maintains a slightly higher Z″ value compared to the CW test sample, thus exhibiting insulating properties. The SW test sample, on the other hand, exhibits fully conductive properties with consistently low values.

Considering electrical and dielectric mechanisms, Z″ values at high frequencies can be considered an indicator of the material's dielectric storage capacity. Therefore, the VW test sample is suitable for applications requiring high energy storage and insulation over a wide frequency range. The SW test sample, with its fast response and high conductivity, offers potential for applications such as humidity sensors and conductive fillers. The CW test sample, on the other hand, exhibits a balanced electrical response profile with intermediate values.

The ε′-ε″ plot for maple wood, shown in Figure 10, examines the real (ε′) and imaginary (ε″) dielectric constants for three different surface conditions (CW, SW, and VW) using three main mechanism regions along the frequency axis. In Figure 10, the yellow region represents interfacial polarization, the blue region represents dipolar relaxation, and the pink region represents the atomic/polar response.

In Figure 10, the ε′–ε″ data of the maple test samples show significant differences depending on the surface modification. The CW test sample has a strong polarization capacity with the highest ε′ values at low frequencies. Conduction-related losses dominate the ε″ curves

at low frequencies, while it exhibits pronounced dipolar relaxation at mid-frequencies. Although the SW test sample has lower ε′ values at low frequencies compared to the CW, it shows high losses in the ε″ curves that extend over a wider frequency range. This indicates that surface roughness increases the conduction paths and broadens the relaxation time distribution. The VW test sample, on the other hand, has the lowest ε′ and ε″ values at low frequencies, while the surface coating limits charge carrier mobility and reduces the polarization capacity. Figure 11 compares the Z′–Z″ Nyquist diagram of the maple test samples for the impedance response under three different (CW, SW, and VW) surface conditions.

The Nyquist Z′–Z″ spectra in Figure 11 show variations with surface conditions, which are consistent with results. The CW test sample exhibits high electrical resistance and strong interfacial polarization in the low-frequency range with a large-radius semicircle, while the SW test sample exhibits lower impedance and a high conductivity contribution with a smaller-radius semicircle. The VW test sample, on the other hand, exhibits high surface resistance and low conductivity with a larger semicircle diameter than the CW and SW test samples. The Z″ axis shows the constant frequency characteristics in the CW and VW models, while the SW model shows the high frequencies with different distributions.

Conclusions

In this study, the dielectric and electrical properties of maple wood were comprehensively investigated over a wide frequency range (100 Hz to 1 MHz) under three different surface conditions—control (CW), water saturation (SW), and varnish coating (VW). A detailed analysis of the basic dielectric parameters, including real and imaginary permittivity (ε′, ε″), dielectric loss factor (tanδ), alternating current electrical conductivity (σac), impedance components (Z′, Z″), capacitance (C), and frequency-dependent conductive energy component (G/ω), was carried out.

The results indicate that surface treatment plays a significant role in determining the electrical behavior of maple wood. Among the tested modes, the SW test samples (water-saturated) exhibited the highest dielectric activity, characterized by significantly high ε′, ε″, tanδ, σac, and G/ω values, especially in the mid-frequency range. This behavior is attributed to increased ionic conductivity and strong orientational polarization due to the presence of water molecules and mobile ions.

Furthermore, the (SW) test samples exhibited low impedance values (Z′, Z″) and prominent dielectric relaxation peaks, indicating rapid charge carrier mobility and high dielectric loss potential, which are highly desirable properties for energy storage and sensing technologies. The measured capacitance values (C) also reached their peak values in this mode, demonstrating superior charge storage capacity. In contrast, coated (VW) test samples exhibited consistently low ε′, ε″, tanδ, and σac values across all frequencies, demonstrating effective suppression of dipole motion and moisture transport. This limits energy storage while also improving insulation and surface stability, particularly under high-frequency electric fields. Untreated (CW) test samples, on the other hand, exhibited moderate performance across all measured parameters, providing a reliable basis for comparative evaluation.

Each surface modification offers specific application potential in different technical areas, depending on its dielectric performance. SW-treated maple wood samples, thanks to their high dielectric constant and conductivity, provide a suitable dielectric platform for flexible and biodegradable capacitors, supercapacitor electrodes in environmentally friendly energy storage systems, moisture-sensitive dielectric sensors, and sustainable insulation materials for low-frequency applications. Meanwhile, lacquer-coated (VW) test samples, thanks to their low dielectric losses and stable insulation behavior at high frequencies, are suitable for applications such as surface protective coatings in electronic systems, low-loss dielectric barrier applications, and moisture-resistant insulation layers in high-frequency environments.

Considering all dielectric parameters, water-saturated maple wood (SW) was found to be the most suitable surface modification for applications requiring high dielectric performance, such as capacitive energy storage, dielectric sensors, and environmentally friendly electronic systems. In contrast, varnish-coated samples (VW) are more advantageous for high-frequency applications where insulation is a priority, thanks to their low losses and stable insulation properties. This study provides a detailed explanation of how the frequency-dependent dielectric response of maple wood varies depending on the surface treatment, scientifically demonstrating the usefulness of this natural material as a renewable and functional component in applications such as sensors, insulation, and energy storage.

Conflict of interest

The author(s) declare(s) that there is no conflict of interest concerning the publication of this article.

Acknowledgements

I would like to express my sincere gratitude to Prof. Dr. Nevzat Çakıcier for his valuable assistance in providing the wooden material used in this study, and to Assoc. Prof. Dr. Ahmet Demir for granting access to the laboratory facilities required for conducting the measurements on the experimental materials.

References

Ayata Ü., Bal B. C., Şahin S. [2019]: Determination of some physical properties and thermal conductivity value of maple (*Acer trautvetteri* Medw.) wood, ISPEC International Conference on Agriculture and Rural Development - II, September 27-29, Kiev, Ukraine, 29-34.

Barsoukov E., Macdonald J. R. [2005]: Impedance Spectroscopy: Theory, Experiment, and Applications, 2nd ed., Hoboken, NJ, USA: Wiley-Interscience.

Bozkurt A. Y., Erdin N. [2013]: Odun Anatomisi, İ.Ü. Orman Fakültesi Yayınları, İstanbul, Turkey.

Bozkurt Y. [1982]: Ağaç Teknolojisi, İstanbul Üniversitesi Orman Fakültesi Yayınları, vol. 2839, no. 296.

Çavuş V., Ayata Ü. [2018]: An investigation on screw holding strength on woods of magnolia tree, maple and chinaberry tree, Furniture and Wooden Material Research Journal, 1(2): 94-102. DOI: 10.33725/mamad.496615.

Demir A. [2025]: Multispectral analysis of photosensitive perovskite-E7 liquid crystal composites: Correlating optical response with electrical properties. Optical Materials, 162: 1-10. DOI: 10.1016/j.optmat.2025.116878

Demir A., Musatat A. B., Kip Ş. Z. [2024]: Investigation of Dielectric Anisotropy and Electrical Modulus-Impedance Properties of PCBM/E7 Composite for Organic Electronic Devices Applications. Celal Bayar Üniversitesi Fen Bilimleri Dergisi, 21(2): 72-79. DOI: 10.18466/cbayarfbe.1562667

Dzurenda L., Geffert A., Geffertová, J., Dudiak M. [2020]: Evaluation of the process thermal treatment of maple wood saturated water steam in terms of change of pH and color of wood. BioResources, 15(2): 2550-2559. DOI: 10.15376/biores.15.2.2550-2559

Gencel O., Musatat A. B., Demir A., Tozluoğlu A., Tutuş A., Kıllı U., Fidan H., Kosovalı Cavuş F. [2024]: Transforming industrial byproduct to eco-friendly functional material: Ground-granulated blast furnace slag reinforced paper for renewable energy storage. Science of the Total Environment, 954: 1-15. DOI: 10.1016/j.scitotenv.2024.176616

Ghildiyal V., Altaner C. M., Heffernan B., Jarvis M. C. [2025]: Electrical Phenomena in Trees and Wood: A Review. Current Forestry Reports, 11(1): 1-17. DOI: 10.1007/s40725-024-00238-0

Hussein A. A., Abdullah R. M. [2017]: Dielectric behavior and functionality of polymer matrix/cigarette butts composites. European Journal of Materials, 5(2), 65–73.

Hussain G., Batool S., Zheng Y., Li S., Wang X. [2022]: Towards multifunctional applications of Fullerene-filled (PVA-PEG) polymeric nanocomposite films: structural, optical, and electrical properties. Materials, 15(18), 6249.

İbrahimoğlu E., Demir A., Çalışkan F., Tatlı Z. [2024]: The dielectric characteristics of spray deposited α-Si_3N_4:ZnO thin films: The nitride effect on frequency-dependent capacitance and conductance profiles. Solid State Sciences, 158: 1-10. DOI: 10.1016/j.solidstatesciences.2024.107754

Kao K.C. [2004]: Dielectric Phenomena in Solids, With Emphasis on Physical Concepts of Electronic Processes. In 1st ed. Amsterdam, Netherlands: Elsevier Academic Press,. DOI: 10.1016/B978-0-12-396561-5.50019-0

Kĭp Ş. Z., Gegïn K., Demïr A., Köysal O., Öztürk S., Kösemen A. [2024]: The novel n-channel liquid crystal organic field effect transistor (LC-n-OFET): A promising technology for low-power electronics. Organic Electronics, 125: 1-8. DOI: 10.1016/j.orgel.2023.106965

Kırkbınar M., İbrahimoglu E., Demir A., Çalışkan F. [2024]: Investigating ultra-thin rGO coated ZnO core-shell structures in MOS devices: Electrical/dielectric characteristics and relaxation mechanism. Materials Science and Engineering: B, 310: 1-9. DOI: 10.1016/j.mseb.2024.117722

Kocakülah G., Köysal O. [2023a]: Conductivity and optical bandgap parameters variations of methyl red-doped 4-pentyl-4′-cyanobiphenyl nematic liquid crystal: norland optical adhesive 65 photopolymer composites. Journal of Materials Science: Materials in Electronics, 34(19): 1–11. DOI: 10.1007/s10854-023-10857-1

Kocakülah G., Köysal O. [2023b]: The Fluorescent Materials Effect on Physical Parameters of Nematic Liquid Crystals. Journal of Electronic Materials, 52(8): 5707-5718. DOI: 10.1007/s11664-023-10522-7

Macdonald J. R. [1992]: Impedance spectroscopy. Annals of Biomedical Engineering, 20, 289-305. DOI: 10.1166/jnn.2011.5092

Mandraveli E., Mitani A., Terzopoulou P., Koutsianitis D. [2024]: Oil heat treatment of wood—A comprehensive analysis of physical, chemical, and mechanical modifications. Materials, 17(10), 2394, 1-22. DOI: 10.3390/ma17102394

Markiewicz E., Paukszta D. [2009]: Dielectric properties of lignocellulosic materials–polypropylene composites. Materials Science, 27(2), 231–237.

Ondo-Ndong R., Essone-Obame H., Moussambi Z. H., Koumba N. [2018]: Capacitive properties of zinc

oxide thin films by radiofrequency magnetron sputtering. Journal of Theoretical and Applied Physics, 12(4): 309-317. DOI: 10.1007/s40094-018-0309-9

Otten K. A., Brischke C., Meyer C. [2017]: Material moisture content of wood and cement mortars – Electrical resistance-based measurements in the high ohmic range. Construction and Building Materials, 153: 640-646. DOI: 10.1016/j.conbuildmat.2017.07.090

Ramazanoğlu D., Subaşı A., Musatat A. B., Demir A., Subaşı S., Maraşlı M. [2025a]: Dielectric property enhancement of glass fiber-reinforced concrete via TiO_2 nanocomposites. Structures, 79: 1-16. DOI: 10.1016/j.istruc.2025.109444

Ramazanoğlu D., Subaşı A., Musatat A. B., Demir A., Subaşı S., Maraşlı M. [2025b]: Multifunctional SnO_2-@ doped glass fiber-reinforced concrete: Improved microstructure, mechanical, dielectric, and energy storage characteristics. Construction and Building Materials, 476: 1-15. DOI: 10.1016/j.conbuildmat.2025.141231

Saeed N. [2022]: Experimental data for thermal conductivity and dielectric properties of wood and wood-based materials. Data in Brief, 42: 1-7. DOI: 10.1016/j.dib.2022.108027

Shabnam T. [2011]: Mechanical and Electrical Properties of Surface Treated Rice Straw Reinforced Polypropylene Composites (Master's thesis). BUET, Bangladesh.

Saini P., Arora M. [2012]: Microwave absorption and EMI shielding behavior of nanocomposites based on intrinsically conducting polymers, graphene and carbon nanotubes. InTech.

Türk Ç. G., Tan S. O., Altındal Ş., İnem B. [2020]: Frequency and voltage dependence of barrier height, surface states, and series resistance in Al/Al_2O_3/p-Si structures in wide range frequency and voltage. Physica B: Condensed Matter, 582: 1-7. DOI: 10.1016/j.physb.2019.411979

Teja P. M. V., Rajyasree C., Rao P. S., Babu A. R., Prasad, A. R. [2012]: Structural and electrical properties of ZnF_2–Bi_2O_3–GeO_2 glasses doped with CoO. Journal of Molecular Structure, 1016(1–3), 68-74.

Varada Rajulu K. C., Mohanty B. N. [2016]: Dielectric and Conductivity Properties of Some Wood Composites. International Journal of Engineering and Technologies, 8: 51-60. DOI: 10.18052/www.scipress.com/ijet.8.51

Výbohová E., Geffertová J., Geffert A. [2018]: Impact of steaming on the chemical composition of maple wood. BioResources, 13(3): 5862-5874. DOI: 10.15376/biores.13.3.5862-5874

Wang C., Zhang Z., Xu X., Wu H., Liu D. [2022]: Flexible and biocompatible polystyrene/multi-walled carbon nanotubes films with high permittivity and low loss. ES Materials & Manufacturing, 17, 45–53.

Wei L., Liu Q. X., Zhu B., Liu W. J., Ding S. J., Lu H. L., Jiang A., Zhang D. W. [2016]: Low-cost and high-productivity three-dimensional nanocapacitors based on stand-up ZnO nanowires for energy storage. Nanoscale Research Letters, 11(213): 1-9. DOI: 10.1186/s11671-016-1429-2

Zhang Z., Zhou H. [2023]: Dielectric characteristics of poplar powder under high-frequency electric field. BioResources, 18(3): 5798-5812. DOI: 10.15376/biores.18.3.5798-5812.

List of standards

ASTM 3023-98:2017 Standard practice for determination of resistance of factory-applied coatings on wood products to stains and reagents, American Society for Testing and Materials, Philadelphia Pa.

ISO, 554: 1976 Standard atmospheres for conditioning and/or testing, International Standardization Organization, Geneva, Switzerland.